RAPID COMMUNICATIONS

PHYSICAL REVIEW B VOLUME 31, NUMBER 6 15 MARCH 1985

Identification of deep-gap states in *a*-Si:H by photodepopulation-induced electron-spin resonance

N. M. Johnson and D. K. Biegelsen
Xerox Palo Alto Research Center, Palo Alto, California 94304
(Received 26 November 1984)

A new technique is described for the microscopic identification of electronic deep levels in semiconductors. Photodepopulation of deep levels is monitored simultaneously with electrical and electron-spin-resonance (ESR) techniques to obtain the distribution of deep levels corresponding to a preselected paramagnetic defect. The technique is demonstrated with combined photodepopulation-induced ESR and photocapacitance measurements on hydrogenated amorphous silicon. The results identify the characteristic Gaussian distribution of midgap states with the distribution of the transition between double and single occupancy of the silicon dangling-bond defect.

Microscopic identification of deep levels in semiconductors requires a combination of complementary techniques which can relate structural and/or chemical information with the electronic or optical properties of a defect. For centers with paramagnetic states, electron-spin resonance (ESR) is a powerful spectroscopic technique for defect identification which has been directly combined with both electrical and optical methods to identify the origin of deep levels. Perhaps the earliest example of this approach was the use of electronic redistribution (by thermal ionization) between *A* centers in crystalline silicon upon removal of uniaxial stress to relate the oxygen-vacancy complex with the deep level at 0.17 eV below the conduction band.[1] Another approach, termed depletion-width-modulated ESR spectroscopy, involved observing changes in the dark absorption ESR signal as a result of modulating the width of the space-charge region in a semiconducting diode of hydrogenated amorphous silicon.[2] The technique relied on thermal ionization of the dangling-bond defect, as detected by ESR, to relate this center with deep levels near midgap, which were measured by deep-level transient spectroscopy. Optical techniques have also been combined with magnetic resonance for deep-level identification. Two examples of this approach are optically detected magnetic resonance[3] and optically detected electron-nuclear double resonance.[4] This Rapid Communication describes a new photoelectric-ESR technique for the microscopic identification of deep levels in semiconductors. Photodepopulation of deep levels is monitored simultaneously with electrical and ESR techniques to obtain the distribution of deep levels corresponding to a preselected paramagnetic defect. The technique is demonstrated with combined photodepopulation-induced ESR and photocapacitance measurements on *a*-Si:H. The results identify the characteristic Gaussian distribution of midgap states with the transition between single and double occupancy of the silicon dangling-bond defect.

The photodepopulation technique is illustrated in Fig. 1 with energy-band diagrams of a Schottky-barrier diode on an *n*-type amorphous semiconductor. The measurement involves cooling the device to a low-temperature T in order to freeze out thermal emission from deep levels while retaining band-tail mediated charge transport and sufficient electrical conductivity for monitoring the capacitance. After a zero-bias voltage plus to populate deep levels with electrons up to the Fermi energy, a reverse bias establishes a layer depleted of free carriers. Illumination with monochromatic light of energy $h\nu$, which is less than the band-gap energy E_G, photoemits electrons that are trapped in the energy interval extending from an energy depth $E_{\rm th}$ to $h\nu$ below the conduction-band mobility edge E_C. The energy $E_{\rm th}$ is the depth to which deep levels are depopulated by thermal emission during the measurement; that is, $E_{\rm th} \equiv k_B T \ln(\gamma_n t_m)$, where k_B is Boltzmann's constant, γ_n is the attempt to escape frequency ($\sim 10^{12}$ sec^{-1}), and t_m is the duration of the measurement.[5] The photoemitted electrons are swept out of the depletion layer without being retrapped by deep levels (for an average electron range which exceeds the depletion width), which leads to an increasing diode capacitance C (decreasing depletion width) with time t. If paramagnetic centers are generated by photodepopulation, then the increasing space-charge density in the depletion layer is accompanied by an increasing spin density $S(t)$, which can be monitored by ESR. Large reverse biases V_R are used to produce large depletion widths W so

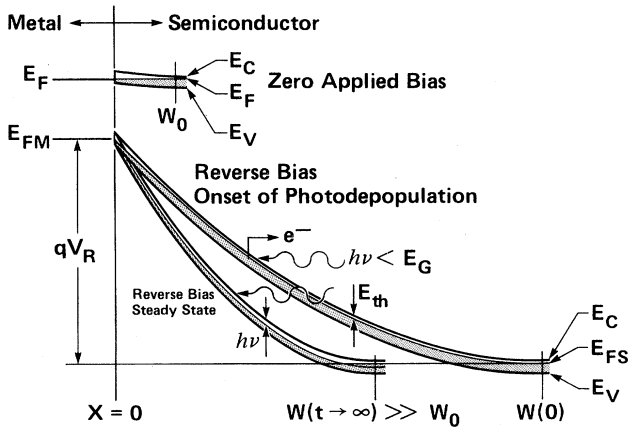

FIG. 1. Energy-band diagrams for a Schottky-barrier diode on an amorphous semiconductor at zero applied bias and under a large reverse bias V_R. The shaded regions signify gap states that are occupied with electrons. For V_R the diagrams display both the onset of photodepopulation, with photon energy $h\nu$ less than the band-gap energy E_G, and steady state. The depletion widths for no applied bias and with V_R are designated W_0 and $W(t)$, respectively.

that there is negligible contribution to the space charge from the zero-bias depletion layer of width W_0 and negligible effect from the Debye tail of free carriers at the edge of the depletion layer.

Ideally, if the illumination is continued for a sufficiently long time, a steady state will be reached in which the gap states are depopulated to a depth $h\nu$ below E_C. In practice several mechanism can preclude this attainment. First, consider optical transitions from deep levels to the localized band-tail states in an amorphous semiconductor. Such transitions are much less probable than those to extended states due to the exponentially decreasing density of states below the mobility edge and the small overlap of the wave functions between initial and localized final states. However, given sufficient time these transitions will contribute to depopulation since electrons excited to band-tail states can be reemitted thermally to extended states and swept out of the depletion layer. This will depopulate gap states to a depth greater than $E_C - h\nu$. Secondly, in a-Si:H current-rectifying devices the maximum reverse bias that could be applied for photodepopulation measurements was found to be severely limited by the onset of high-field charge injection from the rectifying contact which replenished photoemitted charge. This complication for the analysis of photodepopulation data was avoided by recording only the initial time interval of the capacitance transient before sufficient space charge accumulated for significant leakage currents. Finally, on Schottky diodes photon energies greater than the metal-semiconductor barrier height will inject free carriers by internal photoemission which will result in a nonzero steady-state occupancy of deep levels.

Photodepopulation measurements were performed on p^+-n junction diodes. The devices consisted of a 7-μm layer of phosphorus-doped ($[PH_3]/[SiH_4] = 2\times10^{-5}$) a-Si:H sandwiched between thin n^+ and p^+ layers which were contacted with semitransparent metal films. Large-area diodes (0.475 cm^2) were mounted in the microwave cavity of an ESR system and cooled to 132 K. The diode capacitance was monitored at 100 Hz in order to minimize the effect of series resistance. The ESR was monitored with a second-derivative method. The magnetic field was modulated at 33 Hz with the amplitude equal to the separation of the peaks in the first derivative dangling-bond ESR response, and the resulting spin signal was detected with a phase-sensitive amplifier. The dc magnetic field was set by using a known dangling-bond resonance in an undoped a-Si:H sample, and the system gain was determined by using a measured amount of spin-calibrated pitch configured into the sample geometry. Experimental results are illustrated in Fig. 2. The upper and lower waveforms are the time-resolved capacitance and spin density, respectively, which result from periodically applying a zero-bias pulse to a reverse-biased diode while continuously illuminating the diode with sub-band-gap light of low intensity. The transient responses are shown at the beginning and end of a 12-sec pulse period. The waveforms clearly demonstrate that photodepopulation of electronic deep levels is accompanied by photogeneration of paramagnetic centers.

The photodepopulation-induced ESR signal differs in a fundamental way from light-induced ESR (LESR) in a-Si:H. Lightly doped n-type material displays no ESR in the dark. Continuous illumination with sub-band-gap light produces an ESR spectrum which is the superposition of signals from a dangling bond with a g value of 2.0055 and a trapped

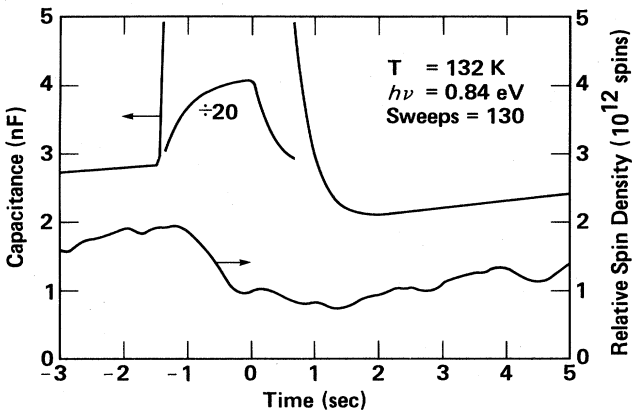

FIG. 2. Simultaneously recorded and time-resolved capacitance and dangling-bond spin density for a p^+-n junction diode with bias $V_R = -39$ V and illuminated with sub-band-gap light of energy $h\nu = 0.84$ eV. The deep-gap states were filled during a zero-bias voltage pulse of 1.4-sec duration, and both signals were monitored with an integration time of 300 msec. The diode temperature was 132 K, and the waveforms are averages of 130 traces.

band-tail electron with $g = 2.0043$.[6] After removing the light, the LESR decays in less than 100 msec (at 130 K) due to recombination of the band-tail electron with the dangling-bond defect.[7] By contrast, the photodepopulation-induced ESR signal persists in the dark under reverse bias, has the dangling-bond g value, and originates from centers in the depletion layer of the device (as is demonstrated in Fig. 2 by collapsing the depletion width with a zero-bias pulse). All of these features are consistent with the phenomenon of defect photodepopulation as depicted in Fig. 1.

The deep-level distribution in n-type a-Si:H has been found to be dominated by an approximately Gaussian-shaped distribution $g_e(E)$ located near midgap.[5,8,9] In addition, the silicon dangling-bond defect has been shown to have states deep in the gap.[2,10] This is an amphoteric defect which can hold zero, one, or two electrons, with the unpaired spin of the singly occupied center responsible for the ESR signal. The $1 \leftrightarrow 2$ electron (D^-) transition, the distribution of which will be denoted as $g_s(E)$, is located above midgap, and the $0 \leftrightarrow 1$ electron transition is ~ 0.4 eV deeper.[2,10,11] The present experiment is designed to determine by direct measurement the relation between $g_e(E)$ and $g_s(E)$ and thereby illustrate the photodepopulation-induced ESR technique for electronic defect identification.

The model for the photodepopulation process assumes a continuous deep-level distribution and is based on the depletion approximation for the space-charge layer. It neglects corrections for both a nonzero W_0 and spatial variations of trap occupancy with trap depth.[5,9] These approximations are satisfactory for large V_R such that $W >> W_0$. Analogous to the case in crystalline semiconductors,[12] the initial slopes of the capacitance and spin-density transients depend on $g_e(E)$ and $g_s(E)$, respectively. During the zero-bias pulse, all gap states up to the Fermi energy are populated with electrons. This places the silicon dangling bonds in the doubly occupied state. Consequently, the initial slope of the spin-density transient is due solely to the D^- transition; the $0 \leftrightarrow 1$ electron transition is not detectable by the initial-slope

method, and, therefore, a complete separation between these two transitions is obtained. In addition, hole emission does not contribute to the initial slopes provided $h\nu < E_G - E_{\rm th}$. The photoinduced change in the space-charge density is proportional to $C^2(t) - C^2(0)$, so that the relevant initial slope for the capacitance transient is

$$\Sigma_C \equiv \left.\frac{dC^2}{dt}\right|_{t=0} = \frac{q\epsilon}{[2(V_{\rm bi}+V_R)]}\Phi\beta\nu\int_{E_C-h\nu}^{E_{\rm th}} g_e(E)M_e^2N_f(E+h\nu)\,dE \quad . \tag{1}$$

Similarly, the density of photoinduced spins within the depletion layer is proportional to $S(t)\times C(t)$, so that the appropriate expression for analyzing the spin-density transient is

$$\Sigma_S \equiv \left.\frac{d(SC)}{dt}\right|_{t=0} = \epsilon\Phi\beta\nu\int_{E_C-h\nu}^{E_{\rm th}} g_S(E)M_S^2N_f(E+h\nu)\,dE \quad . \tag{2}$$

In Eqs. (1) and (2), q is electronic charge, ϵ the silicon permittivity, $V_{\rm bi}$ the built-in potential, Φ the flux density [photons/(cm^2 sec)], β a proportionality constant, ν the frequency of the light, and M_e and M_s the (dipole) matrix elements for optical transitions from initial states of density g_e and g_s, respectively, at energy E to final states of density N_f at $E+h\nu$. For a-Si:H it has been shown that M_e may be treated as an average matrix element which is constant for $h\nu < 3.4$ eV.[13] It will be assumed here that M_s is also a constant.

Results from the initial-slope analysis of the photocapacitance transient are shown in Fig. 3. For this measurement diodes were mounted in a conventional cryostat; this permitted convenient optical alignment and calibration of the incident light intensity, which was corrected for electrode transparency to determine Φ. In Fig. 3 is plotted $2(V_R+V_{\rm bi})\Sigma_C/(q\epsilon\Phi)$, which is the optical absorption as measured by the photocapacitance technique, versus photon energy; it was demonstrated at each energy that the initial slope was linearly dependent on light intensity. In addition, at each energy the intensity was adjusted for a constant Σ_C so that the absorption was linearly proportional to $1/\Phi$. The solid curve in Fig. 3 is the absorption computed from Eq. (1) for the model density of states shown in the inset. An excellent fit is obtained with a Gaussian distribution of gap states which is peaked at $E_C - 0.83$ eV and has a standard deviation of 0.12 eV. However, an uncertainty of ~ 0.1 eV for the location of the mobility edge in the conduction band[13] yields a final peak placement of 0.8–0.9 eV. This agrees with results from other deep-level spectroscopies based on both thermal emission of electrons[5,8] and optical absorption.[11,14] However, Fig. 3 offers the most direct demonstration to date of the essentially Gaussian shape of the gap-state distribution.

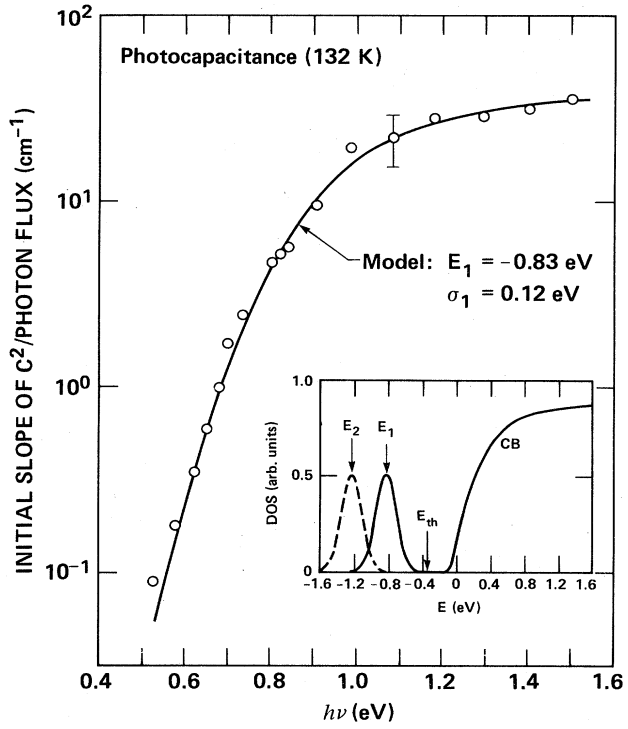

FIG. 3. Initial-slope analysis of the photocapacitance transient for a p^+-n junction diode at 132 K and with $V_R = -39$ V. The zero-bias trap-filling time was 10 sec, and the photodepopulation time was 20 sec for which $E_{\rm th} \approx 0.35$ eV. The error bar denotes the uncertainty of the photon flux density. The inset shows the density of states (DOS), not drawn to scale, used for the model calculation of the photocapacitance. The characteristic deep levels near midgap in a-Si:H are shown as a Gaussian distribution with peak energy E_1 and standard deviation σ_1. For the dangling bond in a-Si:H this distribution may correspond to the $2 \rightleftarrows 1$ electron transition, in which case the dashed-line distribution at E_2 represents the $1 \rightleftarrows 0$ electron transition, which is undetectable by the initial-slope method. The density of conduction-band states (CB) is from Ref. 13.

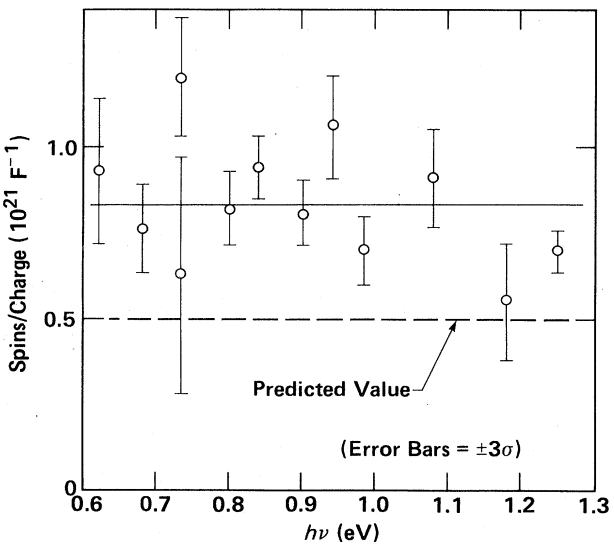

FIG. 4. Ratio of the photogenerated spin density and photoemitted charge density (i.e., Σ_S/Σ_C) vs photon energy $h\nu$ as computed from the initial-slope analysis. The error bars represent plus and minus 3 times the standard deviation σ of a linear least-squares fit to the data. The dashed line is the predicted value of the ratio if all of the characteristic deep levels in a-Si:H are dangling-bond states.

The identity, within experimental accuracy, of $g_e(E)$ and $g_s(E)$ is demonstrated in Fig. 4. This figure shows the quantity Σ_S/Σ_C, which is the ratio of the photodepopulated spin and charge densities in the depletion layer, plotted as a function of photon energy. The large error bars are due to the very weak ESR response, made more extreme by the necessity of working with fractional depopulation. The accuracy of the spin density is limited primarily by the absolute calibration of the ESR and cannot be readily determined to better than a factor ~ 2. The dashed line in Fig. 4 is the predicted value of the ratio specifically for $M_e^2 g_e(E) \equiv M_s^2 g_s(E)$, which from Eqs. (1) and (2) yields $\Sigma_S/\Sigma_C = 2(V_R + V_{bi})/q$. The observed deviation from the predicted value is within the estimated systematic error of the calibration. In addition, at each photon energy SC varied linearly with C^2, with time as the implicit parameter. Thus, the independence of the above ratio on photon energy, the agreement, within experimental uncertainly, between experiment and calculation, and the linearity of SC vs C^2 all demonstrate that the Gaussian distribution of deep-gap states arises from the $1 \rightleftharpoons 2$ electron transition of the silicon dangling bond in a-Si:H.

Combining photodepopulation-induced ESR with photocapacitance or photocurrent measurements should be feasible for identifying deep levels in crystalline as well as amorphous semiconductors. The general requirements may be summarized as follows: an identifiable paramagnetic defect must be present in sufficient concentration in a device configuration for detection by ESR. Issues of compatibility for simultaneous electrical and ESR measurements include fabricating electrically viable devices of large area for spin sensitivity, restrictions on semiconductor conductivity and metal-layer thicknesses for tolerable loading of the microwave cavity, and the detectability of the ESR signal in the temperature range required for electrical measurements, as dictated, for example, by contact or carrier freeze out. The silicon dangling bond in a-Si:H demonstrates the feasibility of satisfying the above criteria for electronic defect identification.

The authors are pleased to thank W. B. Jackson, R. A. Street, and M. Stutzmann for helpful discussions and M. D. Moyer, R. Thompson, and J. Zesch for technical support. The work was partially supported by the Solar Energy Research Institute.

[1]G. D. Watkins and J. W. Corbett, Phys. Rev. **121** 1001 (1961).
[2]J. D. Cohen, J. P. Harbison, and K. W. Wecht, Phys. Rev. Lett. **48**, 109 (1982).
[3]B. C. Cavenett, J. Lumin. **18/19**, 846 (1979).
[4]D. M. Hofmann, B. K. Meyer, F. Lohse, and J.-M. Spaeth, Phys. Rev. Lett. **53**, 1187 (1984).
[5]N. M. Johnson, Appl. Phys. Lett. **42**, 981 (1983).
[6]R. A. Street and D. K. Biegelsen, Solid State Commun. **33**, 1159 (1980).
[7]D. K. Biegelsen, R. A. Street, W. B. Jackson, and R. L. Weisfield, J. Non-Cryst. Solids **66**, 139 (1984).
[8]D. V. Lang, J. D. Cohen, and J. P. Harbison, Phys. Rev. B **25**, 5285 (1982).
[9]N. M. Johnson and W. B. Jackson, J. Non-Cryst. Solids **68**, 147 (1984).
[10]H. Dersch, J. Stuke, and Beichler, Phys. Status Solidi (b) **105**, 265 (1981).
[11]W. B. Jackson, Solid State Commun. **44**, 477 (1982).
[12]A. Chantre, G. Vincent, and D. Bois, Phys. Rev. B **23**, 5335 (1981).
[13]W. B. Jackson, S. M. Kelso, C. C. Tsai, J. W. Allen, and S.-J. Oh, Phys. Rev. B (to be published) .
[14]W. B. Jackson and N. M. Amer, Phys. Rev. B **25**, 5559 (1982).